Coherent Dynamics of Vortex Formation in Trapped Bose-Einstein Condensates

B. M. Caradoc-Davies,[1] R. J. Ballagh,[1] and K. Burnett[2]
[1]*Department of Physics, University of Otago, P.O. Box 56, Dunedin, New Zealand*
[2]*Clarendon Laboratory, Department of Physics, University of Oxford, Parks Road, Oxford OX1 3PU, United Kingdom*
(Received 5 February 1999)

Simulations of a rotationally stirred condensate show that a regime of simple behavior occurs in which a single vortex cycles in and out of the condensate. We present a simple quantitative model of this behavior, which accurately describes the full vortex dynamics, including a critical angular speed of stirring for vortex formation. A method for experimentally preparing a condensate in a central vortex state is suggested.

PACS numbers: 03.75.Fi, 47.32.Cc

The production of vortices has been a central issue in the study of superfluids. It has been demonstrated, for example, that attempts to produce bulk rotation in a cylinder of He II will lead to vortex production, a state which calculations show to be energetically favored. The currently realized [1,2] Bose-Einstein condensates (BEC) offer a new medium for studying vortices, and a number of theoretical studies have considered the properties of static vortices [3,4], their stability [5–8], excitation spectra [9,10], and phase sensitive detection techniques [11]. A variety of methods have been considered by which vortices could be formed in a BEC. Fetter [6] suggested that a rotating nonaxially symmetric trap could imitate the He II rotating cylinder, and obtained an approximate critical rotational speed for vortex production by a heuristic argument. Jackson *et al.* [12] showed that vortices may be generated by movement of a localized potential through a condensate, while Marzlin and Zhang [13] calculated vortex production using four laser beams in a ring configuration. Other numerical simulations, such as collisions of condensates [14,15], have shown in fact that vortex production appears to be a common consequence of mechanically disturbing a condensate.

In this paper, we consider a trapped BEC stirred rotationally by an external potential, and find and analyze a regime where only a single vortex forms. We present a simple quantitative model of this behavior, which accurately describes the full vortex dynamics in terms of a coherent process. The model gives the critical speed of rotation for vortex formation and explains a number of other features that are seen, including the stability of a central vortex (at $T = 0$). Our investigation is based on the Gross-Pitaevskii (GP) equation for the condensate wave function $\psi(\mathbf{r}, t)$,

$$i\,\frac{\partial\psi(\mathbf{r},t)}{\partial t} = -\,\nabla^2\psi(\mathbf{r},t) + V(\mathbf{r},t)\psi(\mathbf{r},t) + C|\psi(\mathbf{r},t)|^2\psi(\mathbf{r},t)\,, \qquad (1)$$

which is known to accurately describe condensates close to $T = 0$. In Eq. (1) we have used scaling and notation as in Ruprecht *et al.* [16]; $V(\mathbf{r}, t)$ is the external potential, and C is proportional to the number of atoms in the condensate and the scattering length. We consider the GP equation in two dimensions only, and solve it numerically. We simulate the effect of stirring by adding to the stationary trap potential a narrow, moving Gaussian potential, representing, for example, a far-blue-detuned laser [17]. $V(\mathbf{r}, t)$ is given by $r^2/4 + W(\mathbf{r}, t)$, and the stirring potential

$$W(\mathbf{r},t) = W_0 \exp\left[-4\left(\frac{|\mathbf{r} - \mathbf{r}_s(t)|}{w_s}\right)^2\right], \qquad (2)$$

is centered at $\mathbf{r}_s(t)$. The initial condensate state for our simulations is the lowest energy eigenstate of the time-independent GP equation [9] in which V includes the stationary stirrer. The stirrer moves anticlockwise on a circular path, accelerating constantly until $t = \pi$, when it reaches its final angular speed ω_f. Figure 1, which shows the state of a condensate after it has been stirred for some time ($t < 5\pi$) then left to freely evolve ($t \geq 5\pi$), illustrates the complexity of behavior that can occur.

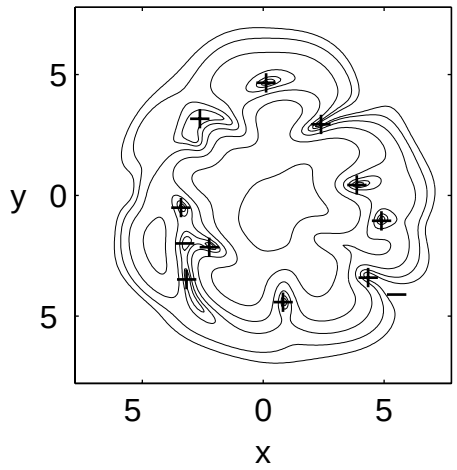

FIG. 1. Probability density at $t = 12\pi$ of a condensate stirred, as described in the text, with the stirrer gradually withdrawn between $t = 4\pi$ and 5π. Contours are logarithmically spaced. Vortices are detected numerically by searching for their 2π phase signature, and are marked near dense regions of the condensate by a + or − sign according to their sense. $C = 88.13$, $\omega_f = 1$, $r_s = 3$, $W_0 = 10$, and $w_s = 1$.

Vortices of positive and negative circulation have formed and, as time progresses, move relative to each other, and annihilate when a positive and negative pair collide [18].

Amidst the complexity of possible behaviors, an important and simply characterized behavior emerges, namely the formation and dynamics of a single vortex. An example which illustrates the main features is given in Fig. 2, where sequential subfigures show the evolution of the condensate as the stirrer revolves. A single vortex enters at the edge of the visible region of the condensate, then cycles to the center of the condensate, and back to the edge. This cycle repeats regularly, as can be seen in Fig. 3 where the solid line shows the angular momentum $\langle L \rangle$ plotted as a function of time for this case. At lower stirring speeds, similar vortex cycling occurs, but with progressively smaller amplitudes as ω_f decreases, so that the vortex oscillates near the condensate edge. We have found that the condensate gains angular momentum even for very small values of ω_f. The *critical angular speed*, which causes a single vortex to cycle right to the center of the condensate, we denote as ω_c. In Table I we present results from our simulations that show that ω_c decreases as C increases, in agreement with the heuristic result of Fetter [6].

The single-vortex behavior can be understood quantitatively in terms of a *nonlinear Rabi cycling* model. The essential idea is that the stirring potential causes the condensate to cycle between the ground state and the first vortex state, analogous to the Rabi cycling of an atom in a light field. We decompose the condensate on the basis of a ground-state-like part (axially symmetric) and a vortex part (axially symmetric with an anticlockwise phase circulation). In the linear (i.e., $C = 0$) limit the condensate would be represented as a superposition of the ground state and the first vortex state of the trap. In the nonlinear system, it is more accurate to decompose the system into collisionally coupled states, in which the radial form of each of the basis states is modified by its collisional interaction with the other. Accordingly we assume that the condensate mean-field wave function can be represented approximately as

$$\psi(\mathbf{r}, t) = a_s(t)\phi_s(r, n_v) + a_v(t)\phi_v(r, n_v)e^{i\theta}, \qquad (3)$$

where r and θ are the cylindrical polar components of $\mathbf{r}$, and $n_v = |a_v|^2$. We obtain the lowest energy coupled eigenstates $\phi_s(r, n_v)$ and $\phi_v(r, n_v)e^{i\theta}$, together with their eigenvalues $\mu_s(n_v)$ and $\mu_v(n_v)$, by solving for a particular value of n_v the coupled time-independent radial GP equations,

$$\mu_\sigma \phi_\sigma = \left[-\frac{1}{r}\frac{d}{dr}\left(r \frac{d}{dr} \right) + \frac{l_\sigma^2}{r^2} + \frac{r^2}{4} + C(n_\sigma \phi_\sigma^2 + 2n_\lambda \phi_\lambda^2) \right] \phi_\sigma . \qquad (4)$$

Here σ and λ are either s or v, $l_s = 0$ and $l_v = 1$ are the angular momenta of ϕ_s and $\phi_v e^{i\theta}$, respectively, n_v is the fraction of the condensate in the vortex component, and $n_s = 1 - n_v$ is the fraction in the symmetric component. The ϕ_σ are real non-negative functions normalized as $\int \phi_\sigma^2 \, d\mathbf{r} = 1$, and ϕ_s and $\phi_v e^{i\theta}$ are of course orthogonal. The superposition in Eq. (3) produces a condensate with an angular momentum expectation value $\langle L \rangle = n_v$, and a vortex whose distance from the center of the trap decreases as $n_v \to 1$. In the absence of a stirrer, the vortex

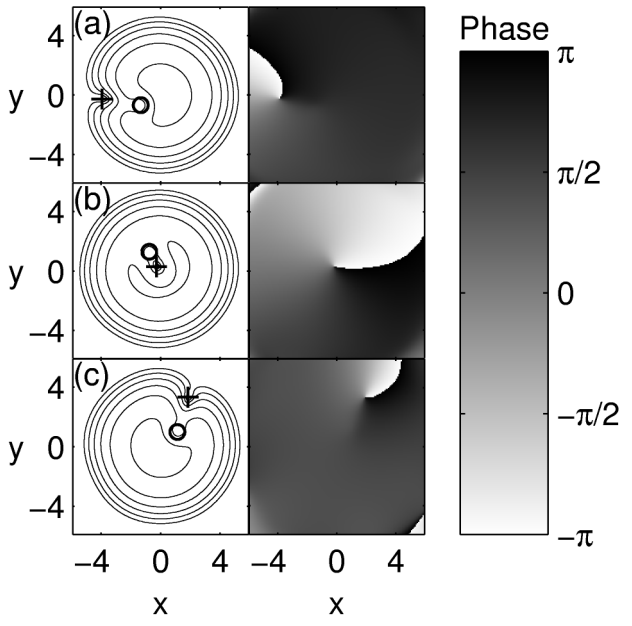

FIG. 2. Sequence of states for a condensate stirred from rest as described in the text. Probability density is shown in the left-hand column, and the phase of ψ in the right-hand column, for (a) $t = 8.80$, (b) $t = 18.35$, and (c) $t = 28.15$. The circle denotes the stirrer. Parameters are the same as in Fig. 1, except $\omega_f = 0.5$ and $r_s = 1.5$.

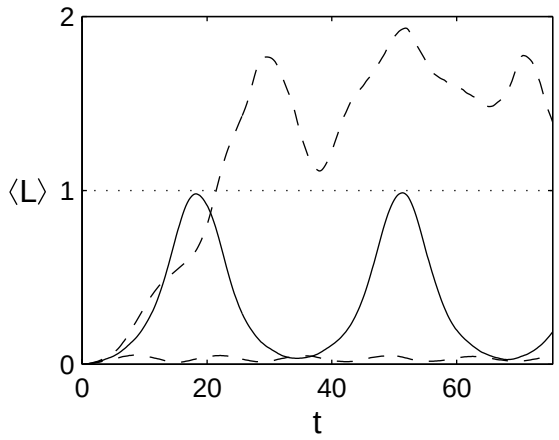

FIG. 3. Angular momentum expectation values versus time for $\omega_f = 0.5$ (solid line), $\omega_f = 0.4$ (lower dashed line), and $\omega_f = 0.6$ (upper dashed line). Other parameters are the same as in Fig. 2.

TABLE I. Critical angular frequency ω_c for the two-dimensional condensate. The final column gives bounds for ω_c found from our simulations of the full GP equation.

C	E_g	E_v	ω_c	Simulation ω_c
0	1	2	1	...
30	1.811	2.520	0.709	0.6–0.8
88.13	2.744	3.284	0.540	0.5–0.6
500	6.079	6.394	0.315	...
5000	18.860	19.000	0.140	...

precesses about the center of the condensate at a frequency $\mu_v - \mu_s$. Substituting Eq. (3) into Eq. (1), and projecting alternately onto the states ϕ_s and $\phi_v e^{i\theta}$, we obtain a pair of coupled equations for $\dot{a}_s$ and $\dot{a}_v$. Noting that a constantly rotating stirring potential $W(\mathbf{r}, t)$ can be written $e^{-i\omega_f t L} W'(\mathbf{r}) e^{+i\omega_f t L}$, and writing $\tilde{a}_s = a_s e^{i\alpha_s}$, $\tilde{a}_v = a_v e^{i(\alpha_s + \omega_f t)}$, where $\alpha_s(t) = \int_0^t \mu_s(t')\, dt'$, we collect the oscillating exponential time dependences and transform to a frame which rotates with the stirring potential to obtain the following equations:

$$\frac{d\tilde{a}_s}{dt} = -i\delta_s(n_v)\tilde{a}_s - \frac{i}{2}\Omega(n_v)\tilde{a}_v\,, \tag{5a}$$

$$\frac{d\tilde{a}_v}{dt} = -i[\Delta(n_v) + \delta_v(n_v)]\tilde{a}_v - \frac{i}{2}\Omega^*(n_v)\tilde{a}_s\,. \tag{5b}$$

Here $\Delta(n_v) = \mu_v(n_v) - \mu_s(n_v) - \omega_f$ and

$$\delta_\sigma(n_v) = \int \phi_\sigma(n_v) W'(\mathbf{r}) \phi_\sigma(n_v)\, d\mathbf{r}\,, \tag{6a}$$

$$\Omega(n_v) = 2\int \phi_s(n_v) W'(\mathbf{r}) \phi_v(n_v) e^{i\theta}\, d\mathbf{r}\,. \tag{6b}$$

Equations (5) formally resemble the classic Rabi equations, and hence we identify the δ_σ as frequency shifts and Ω as the bare Rabi frequency, but note that here these quantities are variable and depend on the value of n_v. Despite this nonlinear dependence, the concept of Rabi cycling provides a simple framework in which to understand the formation and dynamics of a single vortex: the stirring potential couples and causes cycling between the initial ground state and the first excited vortex state. The energy E' in the frame rotating with the stirrer (obtained from the expectation value of $H' = H - \omega_f L$, where H is the lab frame Hamiltonian and L is the dimensionless angular momentum operator) is conserved, and thus in any solution to Eqs. (5), $\tilde{a}_s$ and $\tilde{a}_v$ must follow a trajectory that conserves E'. Complete cycling of the vortex to the center of the condensate occurs when n_v reaches the value of 1, but this requires the energies in the rotating frame of the ground state $\phi_s(r, n_v = 0)$ and the first excited vortex state $\phi_v(r, n_v = 1)e^{i\theta}$ to be equal. Thus the critical angular speed ω_c is given by the relation

$$E_v - \omega_c = E_g\,, \tag{7}$$

where E_g and E_v are the lab frame energies of the ground state and first excited vortex state, respectively. A finite stirrer shifts these energies by $\delta_s(n_v = 0)$ and $\delta_v(n_v = 1)$, respectively, adjusting ω_c by their difference.

In Table I we list the critical angular speeds predicted by Eq. (7) for a range of C values, along with the values of ω_c found from our numerical simulations of the full GP equation for $C = 30$ and $C = 88.13$ cases. The agreement between the predictions from the two-state model and the full numerical simulation is excellent.

It is difficult to obtain accurate simulations at large values of C for numerical reasons. The $C = 0$ case is easily tractable, and although no visible vortex cycling occurs below $\omega_f = 0.25$, a multiple vortex regime is entered at $\omega_f = 0.8 < \omega_c$; the reason being, as Marzlin and Zhang [13] have noted, that the trap levels are equally spaced for the linear case, so that mixing to higher vortex states readily occurs, and our two-state model is no longer valid. The success of the two-state model is dependent on the fact that, for $C \neq 0$, the spacing of the levels is nonuniform.

The Rabi model also allows us to explain other features of the behavior, such as the period of cycling, the response to smaller stirring speeds, and the effect of different values of stirring radius r_s. In Fig. 3 the condensate response to stirring just below the critical speed is shown, and reveals an increase in oscillation frequency and decreased transfer to the pure vortex state, compared to the critical case. In a simple Rabi model, where the detuning Δ and Rabi frequency Ω are constant, the cycling frequency is $\Omega' = \sqrt{\Omega^2 + \Delta^2}$, and the maximum value of n_v is $(\Omega/\Omega')^2$. By identifying the effective detuning for the two-state system to be $\Delta + \delta_v - \delta_g$, these expressions give a qualitative description of the subcritical stirring in Fig. 3. A more quantitative treatment requires the nonlinear character of Eqs. (5) to be taken into account, which is achieved by solving the coupled pair in Eq. (4) to find the eigenvectors and eigenvalues at each value of n_v and then using these to solve Eqs. (5). We note that in Eq. (4) the term $2n_\lambda\phi_\lambda^2$ gives rise to an energy barrier between the $n_v = 0$ and $n_v = 1$ states of the system. The constraint on the system imposed by the ansatz of Eq. (3) increases this energy barrier slightly compared to the true (unconstrained) case, and the accuracy of our procedure can be improved by decreasing this factor of 2. For example, at $C = 88.13$, if we decrease the factor of $2 \rightarrow 1.58$, our two-state model produces behavior which closely matches the results from the full GP equation, as we show in Fig. 4. The energy barrier is deformed by the presence of the stirrer, allowing the system to cycle between the vortex and ground state. If the stirrer is far from the center of the condensate, or is weak, then Ω may be too small to distort the energy barrier sufficiently, and only incomplete cycling occurs even when $\omega_f = \omega_c$. This feature of the nonlinear system, which agrees with our $r_s = 3$ simulations of the full GP equation, is in contrast to the ordinary Rabi

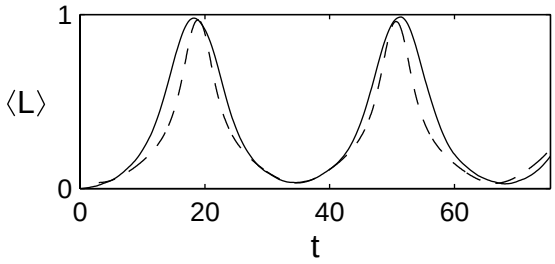

FIG. 4. Angular momentum versus time for the full GP equation simulation (solid line) and the two-state model (dashed line). The two-state model starts at $t = 3$ with $\tilde{a}_s = \sqrt{0.965}$ and $\tilde{a}_v = -\sqrt{0.035}$. Parameters are the same as in Fig. 2.

case, where complete cycling occurs on resonance for any nonzero coupling field.

The validity of the two-state model breaks down when ω_f exceeds ω_c, because then higher energy vortex eigenstates are energetically permitted and mixed into the state of the system, as seen, for example, in Fig. 1 and the upper dashed curve of Fig. 2.

The Rabi model provides some insight into the issue of the stability of a central vortex state [5,10]. We have tested this stability in the $T = 0$ limit by simulation of the GP equation, taking the first excited $l = 1$ vortex state and inserting and withdrawing a narrow stirrer at a fixed location in the laboratory frame. We find that, although the condensate then wobbles vigorously, the vortex undergoes only a very stable small-amplitude oscillation about the trap center [18]. We can interpret this as Rabi cycling of very large effective detuning (i.e., $\omega_f = 0$), and consequently very small transfer probability out of the initial vortex state.

The regular cyclic single-vortex behavior we have found also suggests an experimental technique for preparing a condenstate in a central vortex state. By stirring a condensate for a half-cycle, a vortex will be drawn into a nearly central position.

In conclusion, we have given a simple, quantitative analysis of the single-vortex regime of a stirred condensate. Our two-state model captures the essential coherent dynamics, and accurately predicts the major features of this regime, but also provides a qualitative understanding in terms of the concepts of the well-known Rabi model. Our result for the critical angular frequency can be qualitatively related to that for a rotating cylinder of He II. However, in our case the condensate is inhomogeneous, and the trapping potential plays a central role, giving rise to well-separated condensate eigenstates, of which only the lowest two become significantly involved. It is worth remarking that the speed of sound in the vicinity of the perturber has no relevance to the generation of vortices, in the scenarios we consider here. The model is also easily generalizable to an arbitrarily shaped stirring potential, including a rotating anisotropic potential. Our numerical calculations have been carried out in two spatial dimensions, but can be expected to apply to "pancake" condensates, where the dynamics in the axial direction are frozen out by very tight axial confinement. Qualitative features of our results may have even greater generality, since the two-state model has no direct dependence on dimensionality, and will apply in three dimensions if the system symmetry confines the stirrer to couple the ground state primarily to a single-vortex state.

We thank P. B. Blakie, C. W. Gardiner, and S. Morgan for valuable discussions. This work was supported by The Marsden Fund of New Zealand under Contract No. PVT603.

[1] M. H. Anderson *et al.*, Science **269**, 198 (1995).
[2] K. B. Davis *et al.*, Phys. Rev. Lett. **75**, 3969 (1995).
[3] F. Dalfovo and S. Stringari, Phys. Rev. A **53**, 2477 (1996).
[4] D. A. Butts and D. S. Rokhsar, Nature (London) **397**, 327 (1998).
[5] D. S. Rokhsar, Phys. Rev. Lett. **79**, 2164 (1997).
[6] A. L. Fetter, in *Recent Progress in Many-Body Theories*, edited by D. Neilson and R. F. Bishop (World Scientific, Singapore, 1998), pp. 302–307.
[7] A. L. Fetter, J. Low Temp. Phys. **113**, 189 (1998).
[8] A. A. Svidzinsky and A. L. Fetter, Phys. Rev. A **58**, 3168 (1998).
[9] R. J. Dodd, K. Burnett, M. Edwards, and C. W. Clark, Phys. Rev. A **56**, 587 (1997).
[10] A. A. Svidzinsky and A. L. Fetter, cond-mat/9811348.
[11] E. L. Bolda and D. F. Walls, Phys. Rev. Lett. **81**, 5477 (1998).
[12] B. Jackson, J. F. McCann, and C. S. Adams, Phys. Rev. Lett. **80**, 3903 (1998).
[13] K.-P. Marzlin and W. Zhang, Phys. Rev. A **57**, 4761 (1998).
[14] R. J. Ballagh, T. F. Scott, K. Burnett, and B. M. Caradoc-Davies, Poster presented at *Bose-Einstein Condensation in Atomic Vapors,* Castelvecchio Pascoli, Italy, 1997.
[15] B. Jackson, J. F. McCann, and C. S. Adams, cond-mat/9901087.
[16] P. A. Ruprecht, M. J. Holland, K. Burnett, and M. Edwards, Phys. Rev. A **51**, 4704 (1995).
[17] M. R. Andrews *et al.*, Science **275**, 637 (1997).
[18] MPEG movies showing these results are available from (http://www.physics.otago.ac.nz/research/bec).